Phase-averaged measurements of perturbations introduced into boundary layers

By J. H. Watmuff

1. Motivation and objectives

Large-scale structures in turbulent and transitional wall-bounded flows make a significant contribution to the Reynolds stress and turbulent energy. The objective of this study is to examine the behavior of these structures. Small perturbations are introduced into a laminar and a turbulent boundary layer to trigger the formation of large-scale features. Both flows use the same inlet unit Reynolds number, and they experience the same pressure gradient history, i.e. a favorable (FPG) followed by an adverse pressure gradient (APG). The perturbation consists of a small short duration flow repetitively introduced through a hole in the wall located at the C_p minimum. Hot-wire data are averaged on the basis of the phase of the disturbance, and automation of the experiment has been used to obtain measurements on large spatially dense grids. In the turbulent boundary, the perturbation evolves into a vortex loop which retains its identity for a considerable streamwise distance. In the laminar layer, the perturbation decays to a very small magnitude before growing rapidly and triggering the transition process in the APG. The "time-like" animations of the phase-averaged data are used to gain insight into the naturally occurring physical mechanisms in each flow.

2. Background

2.1 Design of the DNS validation boundary layer experiment

The pressure gradient was specially designed to create an APG turbulent boundary layer with a high enough R_e to sustain turbulence and allow accurate experimental measurements, but low enough for Direct Numerical Simulations (DNS) using a newly developed "fringe" method by Spalart. The design incorporates a region of FPG just downstream of the trip (experiment) or inflow boundary (DNS) to let the flow develop without unduly increasing the local R_e. The pressure-gradient parameter β then rises from about about -0.3 to about +2 within the region accessible to the simulation. The APG flow is far from "equilibrium" and, therefore, represents a significant challenge for DNS. The streamwise extent of the measurements exceeds the current capabilities of direct simulations, and the results are also serving as a useful data base for Reynolds-averaged boundary layer prediction methods. The properties of the unperturbed layer have been documented by Watmuff (1989).

2.2 Automation of the experiment

In the DNS validation experiment, closely spaced profiles were required in the FPG to examine the asymptotic approach to self-similarity and in APG where there

is rapid growth with streamwise distance. A sophisticated high-speed computer-controlled 3D probe positioning system was integrated into the wind tunnel. A considerable investment in both hardware and software enabled all experimental functions (including crossed-wire calibration) to be totally automated under computer control. During the course of the DNS validation experiment, the operation of the facility was refined to the point where experiments could be performed continuously (24 hours a day) over several weeks without manual supervision.

2.3 Phase-averaging technique

An illustrative way of obtaining information about the large-scale motions of turbulent flows is to take averages on the basis of phase. For example, Reynolds and Hussain (1972) used a phase-averaging technique to look at the large-scale motions in a turbulent boundary layer which was excited by vibrating ribbons. Kovaznay, Fujita and Lee (1974) repeatedly produced a turbulent puff from a loud speaker and conditionally sampled the data on the basis of phase. More recently, Cantwell and Coles (1984) and Perry and Watmuff (1981) pioneered flying the hot-wire technique for examining the large-scale features in turbulent wakes. The primary motivation for flying the wires is to avoid hot-wire directional ambiguity in regions of large turbulence intensity or reversed flow. Another advantage of flying the wires is that the data can be obtained on spatially dense grids, allowing large-scale features to be examined in detail. This latter capability can also be exploited using the automated facility, i.e. the phase-averaging technique can applied to an extremely large number of grid points by performing the measurements on a point-by-point basis.

3. A vortex loop introduced into the APG turbulent layer

3.1 Experimental technique

Phase-averaged (64 phase-interval) velocity and Reynolds stress measurements have been made in the DNS validation boundary layer based on the phase of a small disturbance repetitively introduced into the flow. The disturbance consists of a short duration flow from a 0.6mm diameter hole located on the centerline of the test plate at the C_p minimum. The flow was initiated by a rubber diaphragm driven by a small electromagnetic shaker. By examining data taken at single points while tuning the duration, magnitude, and frequency (repetition rate) of the flow from the hole, it was discovered that even with a relatively small perturbation, phase-averaged data could be extracted 0.45m downstream, although the washout was quite severe and some smoothing was required. The magnitude and duration (3.5 msec) of the disturbance were fixed such that the flow from the hole penetrated only to about 8mm into the boundary layer ($\delta \approx 12$mm). A frequency of 40Hz ensured that the streamwise distance between the regions influenced by the disturbance was large enough (approximately 0.15m) to prevent mutual interaction during the downstream motion.

Measurements have been obtained at over 5000 grid points on the centerline plane and five cross-stream planes. The data were reduced on-line and consist of phase-averaged velocities, Reynolds stresses at constant phase and temporal mean

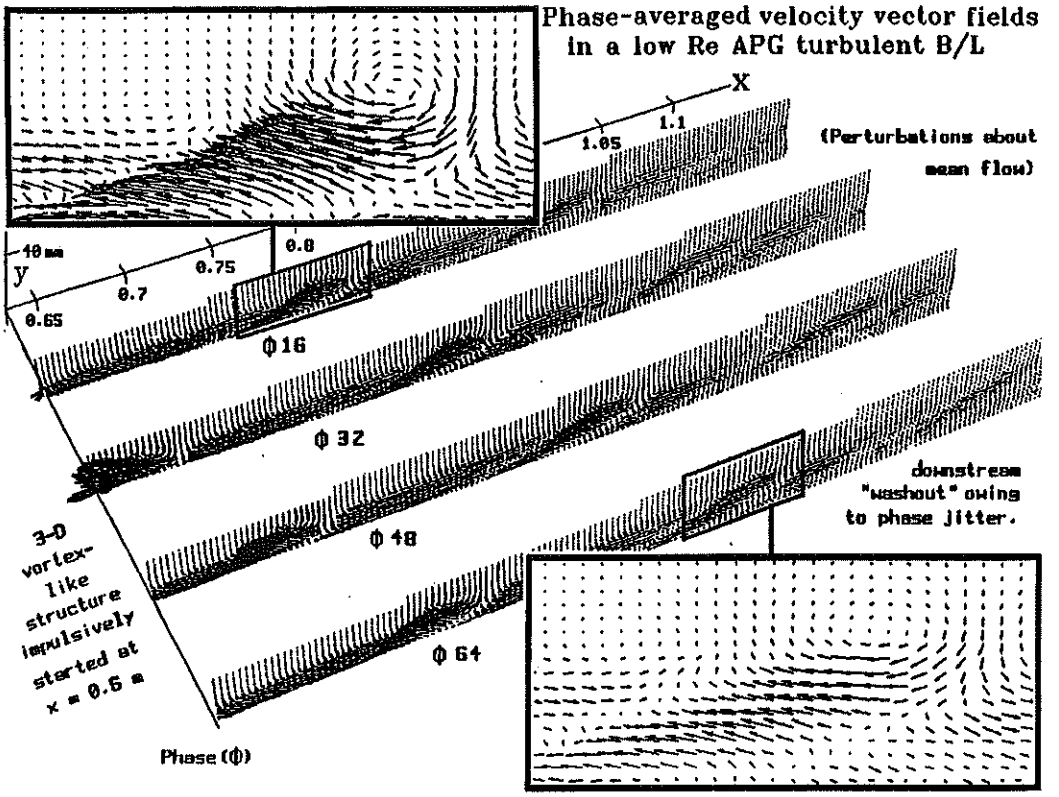

FIGURE 1. Phase-averaged perturbation velocity vector fields in centerline plane of adverse pressure gradient turbulent boundary layer.

velocity, and Reynolds stresses which were all calculated from the same raw hot-wire voltages. Over 1.5×10^5 samples were used for the averages (2400 per phase interval) at each grid point over a sampling period of 60 seconds. About 300 hours of experimental run-time of the automated system were required.

3.2 Interpretation of flow patterns

The velocity vectors in the vicinity of the hole have a "mushroom" shape, characteristic of a vortex-ring. About 50mm downstream of the hole, the strength of the phase-averaged streamwise velocity perturbations is quite small, i.e. about 3% of the local temporal mean velocity. The flow pattern is barely discernible in the streamwise plane when viewed in a frame of reference moving with the perturbations because of the mean shear. However, vortex-like flow patterns appear in the *perturbation* velocity vector fields for the centerline plane as shown in figure 1. The four (out of a total of sixty-four) vector fields are plotted using phase as the third coordinate. The perturbation flow pattern occupies the full height of the layer. Details can be seen in the two small regions which have been plotted using a larger scale. A thin region trails behind the vortex-like pattern where the gradients of the

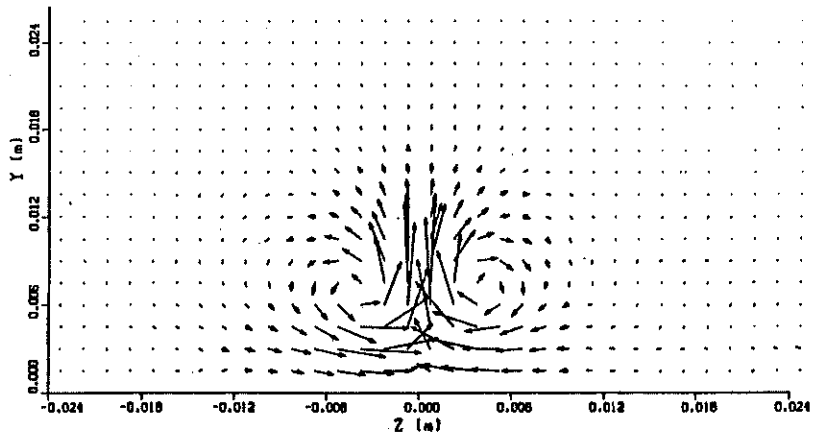

(a)

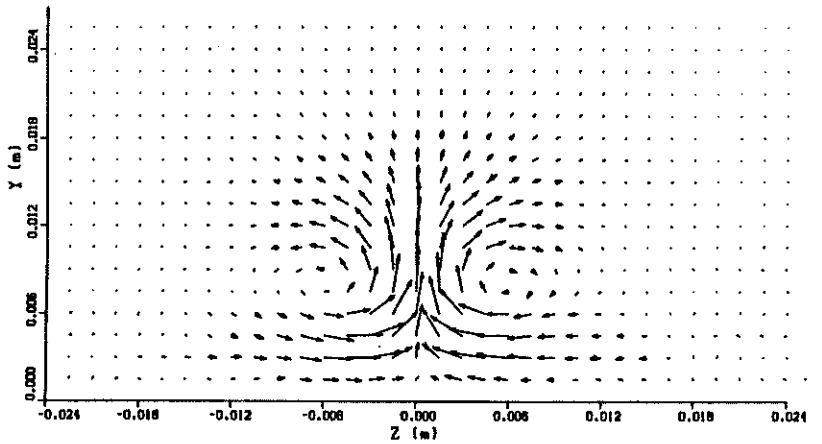

(b)

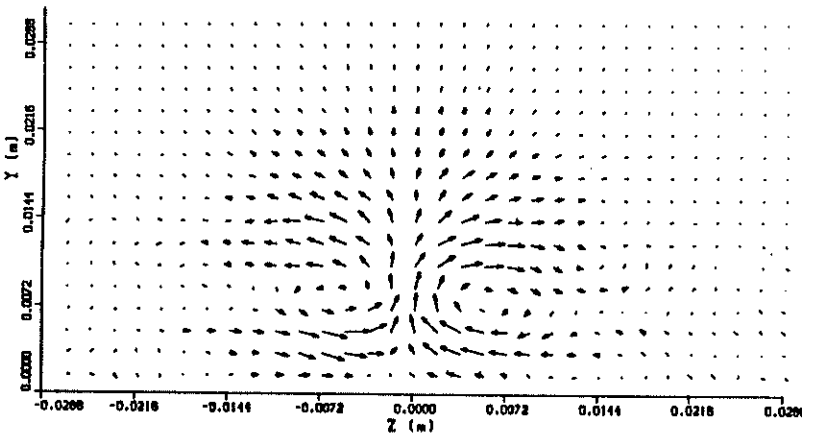

(c)

FIGURE 2. Phase-averaged vectors in spanwise yz-planes located at (a) X=0.651m, (b) X=0.702m, (c) X=0.804m.

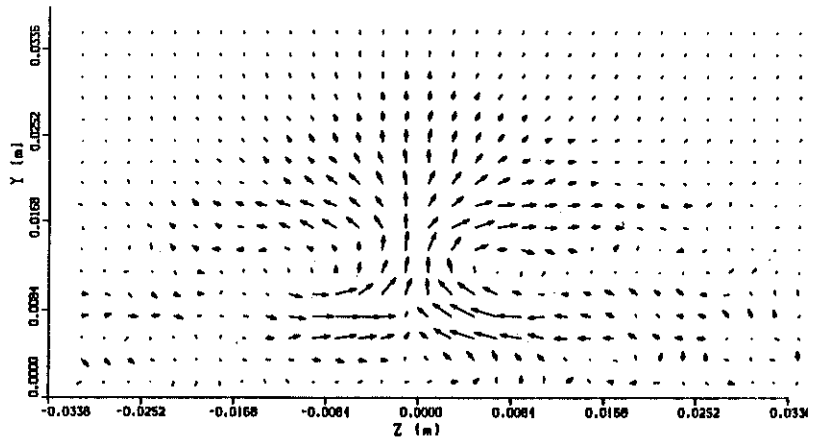

(d)

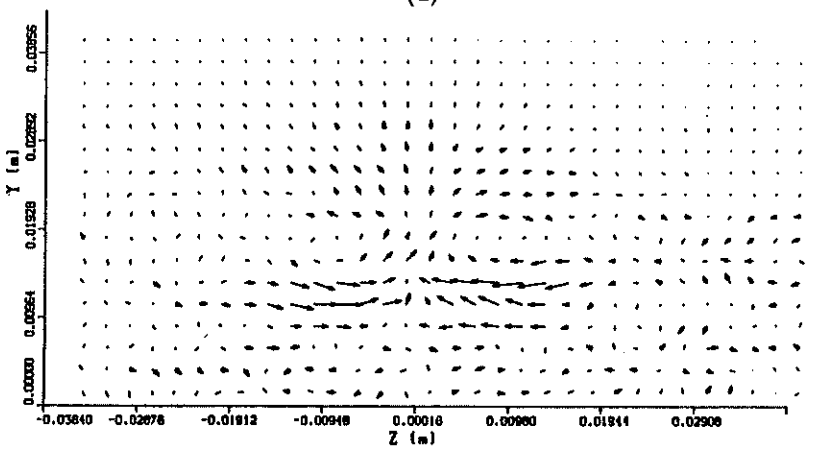

(e)

FIGURE 2. (continued) Phase-averaged vectors in spanwise yz-planes located at (d) X=0.906m (e) X=1.008m.

velocity perturbations are very large. This region is inclined at about 30° to the wall. By about 0.45m downstream of the hole, the strength of the velocity vectors decays to less than 1/2% of the mean velocity owing to phase jitter. However, the same characteristic flow pattern is still discernible in the perturbation vectors, i.e. the loop retains its identity for at least 30δ in the streamwise direction.

The mean shear does not obliterate the pattern in the spanwise planes, and two counter rotating vortex-like motions can be seen in figures 2(a)-(e). Animation of the spanwise vector fields shows that the patterns move apart and towards the wall as the pattern in the streamwise plane passes through. Three-dimensional data have been created by applying Taylor's Hypothesis to each of the spanwise planes. Contours of perturbation vorticity magnitude corresponding to the second spanwise plane are shown in figure 3. The contours provide convincing evidence that the perturbation has evolved into a vortex-loop.

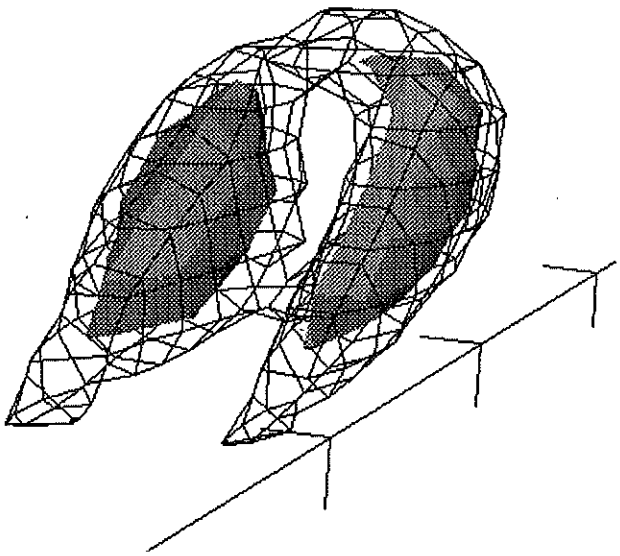

FIGURE 3. Contour surfaces of vorticity magnitude obtained by applying Taylor's Hypothesis to spanwise plane at X=0.702m in turbulent boundary layer.

3.3 Other results

Spanwise Preston tube C_f measurements are within $\pm 1.5\%$ whether the impulsive disturbance is on or whether it has been turned off, even very close to the hole. The centerline mean velocity and Reynolds stress profiles are the same (within the experimental uncertainty) except in the vicinity of the hole. Further, the presence of the disturbance does not alter the power spectral density in the region downstream of the hole. A spectrum analyzer set for a 5Hz span centered around the disturbance frequency showed the same spectra even when 256 rms averages were used. These observations suggest that the phase-averaged vortex-loop could be representative of the behavior of naturally occurring vortex-loops in APG turbulent boundary layers.

3.4 Discussion

The observations could act as a guide for the formulation of physical models of boundary layer turbulence. For example, the model of wall turbulence proposed by Perry and Chong (1982) is physical in the sense that distributions of Λ-vortices are used to explain the mean flow, Reynolds shear stress, and turbulence intensities observed in experiments. Turbulence spectra having all the correct properties were derived from the velocity signatures of the potential-flow vortices. Various scenarios were considered in the formulation of the model such as pairing of the Λ-vortices. Another possibility considered by Perry and Chong is one in which the eddy continuously draws vorticity from the viscous sublayer as it moves downstream.

The phase-averaged vortex-loop study tends to support the latter scenario. The sublayer vorticity in the APG decreases by a factor of 2 in the region covered by the phase-averaged measurements. If vortex-loops do continuously draw up sublayer

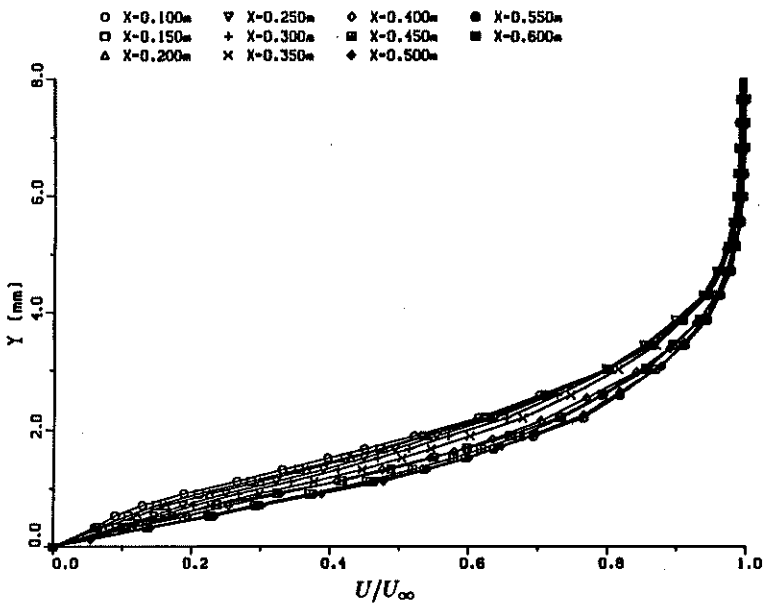

FIGURE 4. Development of laminar velocity profiles in FPG.

vorticity, then the axial vorticity distribution along the loop is likely to increase with wall distance in the APG since the vorticity at greater distances from the wall would have originated from further upstream. The two counter-rotating vortex-like motions in the most downstream spanwise plane are stronger when they are far from the wall, and this is consistent with the above conjecture. Of course, vortex-stretching and other dynamical phenomena would modify the axial vorticity distribution. Nevertheless, increasing axial vorticity of vortex loops with increasing wall distance provides a plausible physical explanation for the bulging of peak values of turbulence intensities away from the wall that are observed in APG layers.

4. Boundary layer transition in an adverse pressure gradient

4.1 Introduction

Emmons (1951) proposed that transition from laminar to turbulent flow occurs through the generation, growth, and amalgamation of turbulent spots. It has been suggested (e.g. Schubauer and Klebanoff 1956) that spots are dynamically similar to turbulent layers, but simpler, so that their study could provide insight into the physical processes occurring within turbulent boundary layers. This suggestion has motivated many investigations into the nature of turbulent spots.

Previous studies have been performed in nominally zero pressure gradients and have used rather large disturbances (e.g. an electric spark as well as flow from a hole in the wall) to force spot formation to occur close to the source of the disturbance. Often, natural spot formation was not observed when the disturbance

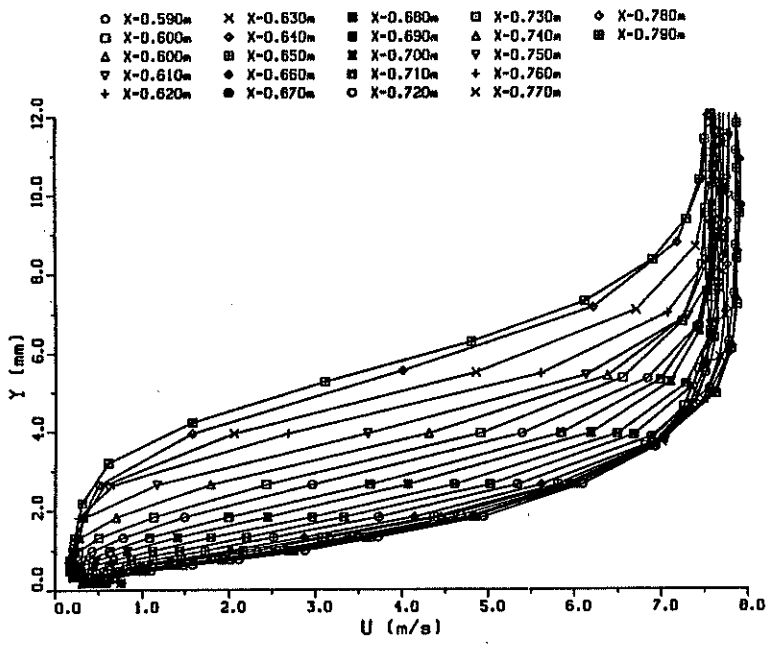

FIGURE 5. Development of laminar velocity profiles in APG.

was removed, even very far downstream, e.g. in the study of Cantwell, Coles and Dimotakis (1978), the unforced layer remained laminar along the entire test section length. Perry, Lim and Teh (1981) observed that too strong a disturbance changes the initial character of a spot, but that it "would look much the same as any other spot" after sufficient development. However, the observations of Perry *et al.* were made for a single location of the disturbance, and measurements were not made, so it is uncertain whether the downstream character of a spot is truly independent of the nature of its formation. Further, it is uncertain whether spots generated in laminar layers which are far from instability are representative of spots that form as part of the natural transition process.

4.2 Experimental technique

Removal of the trip wire while maintaining the same wing-like pressure distribution and inlet unit Reynolds number as in the DNS validation experiment leads to a laminar boundary layer which undergoes natural transition about 0.2m downstream of the C_p minimum. Perry *et al.* reported that attempts to produce identical spots using periodic disturbances failed and suggested that phase-averaged hot-wire measurements would simply result in a "big-eddying-type" of description because of the phase jitter and associated washout. However, examination of hot-wire signals in the vicinity of natural transition in the APG revealed that extremely complex signals could be generated in a very repetitive manner by initiating a short duration flow from the hole located at the C_p minimum (where $\delta \approx 6$mm, $U_\infty \approx 7.5$

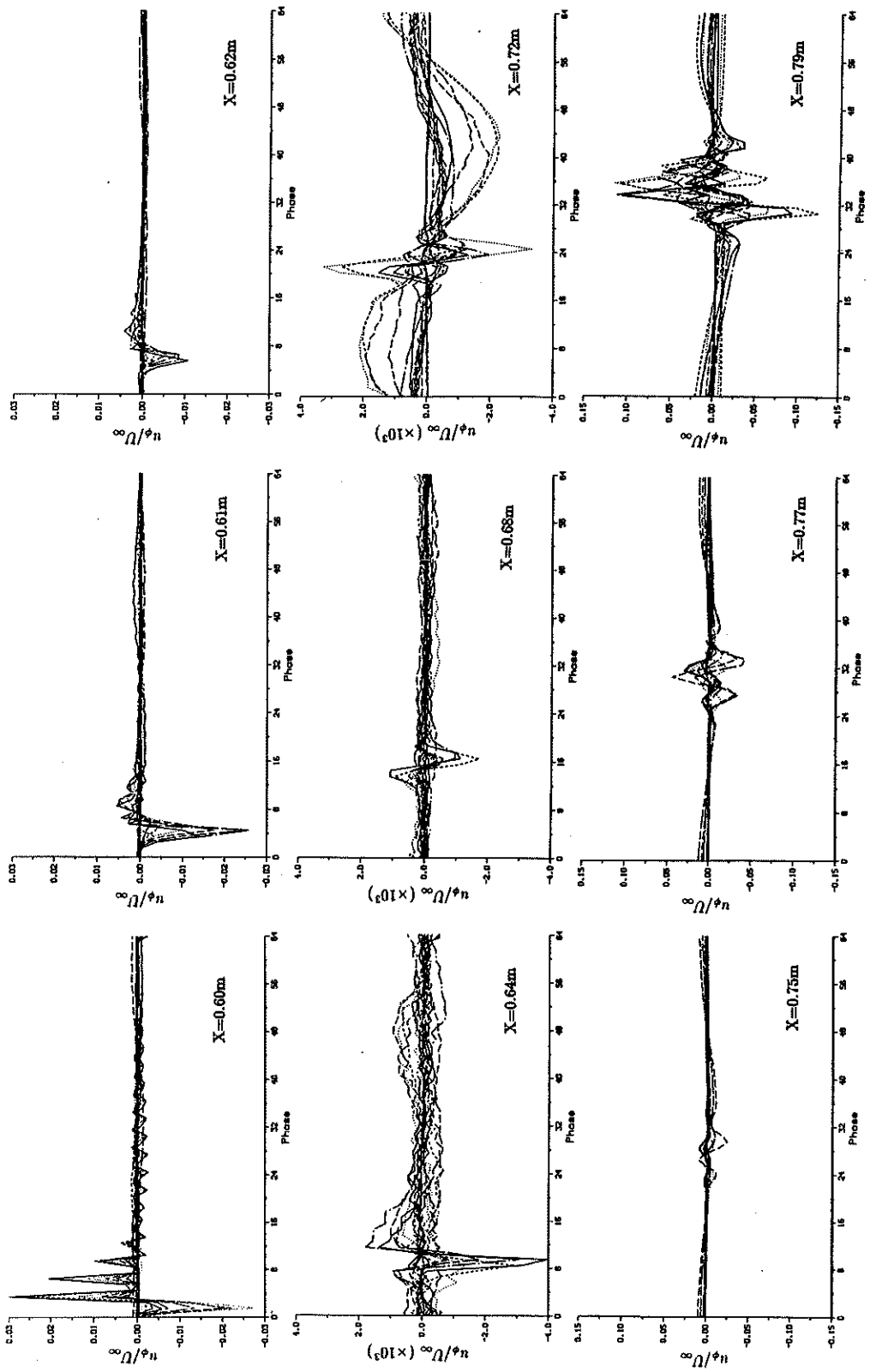

FIGURE 6. Evolution of phase-averaged streamwise velocity perturbations in adverse pressure gradient laminar layer.

m/s). The laminar layer develops severe inflection points in the APG leading to the formation of a strong shear layer close to the wall. As shown below, the repetitive signals are the result of rapid growth of waves developing on the shear layer which ultimately lead to the formation of a spot-like flow containing vortex-loops.

Signals with a wide variety of characteristics can be produced at a fixed position by adjusting the magnitude and duration of the flow. For example, when the magnitude of the impulsive-like flow is small and its duration is 3 msec, the rapid growth of the instability occurs only 25mm upstream of the point of natural transition. Under these conditions, the injected fluid is barely detectable in the laminar layer and then only very close to the wall. Further downstream, the hot-wire signals appeared to be fully turbulent and oscilloscope traces seemed to be uncorrelated with the disturbance. However, cursory measurements indicated that phase-averaged data could be extracted far downstream of the transition region.

The extremely repetitive formation process meant that phase-averaged crossed-wire measurements could be used to examine detailed motions. The disturbance frequency must be low enough to allow the downstream flow to recover between the passage of successive instabilities. However, too low a frequency is undesirable because the phase resolution would be insufficient. Lower frequencies also means a longer time for a given number of cycles, increasing the total experimental run-time. A maximum generating frequency was determined by examining hot-wire signals at a number of points close to the wall downstream of the transition region. The signals at points closest to the wall required the longest time to recover from the transients. High generation frequencies (e.g. 20Hz) did not allow the transients to decay sufficiently, and this altered the character of the signals (i.e. the structure of the flow). A frequency of 8Hz was finally selected for performing a detailed study. The signals observed for this disturbance frequency were the same as those produced by using much lower frequencies (e.g. 1Hz) while allowing very nearly the same degree of recovery from transients. Phase-averaged (64 interval) crossed-wire (UV-orientation) measurements of velocity and Reynolds stress as well as temporal mean velocity and Reynolds stress have been measured on a number of planes. The centerline streamwise plane normal to the wall (250 X by 17 Y positions= 4250 grid points) was measured only with the UV-orientation of the crossed-wire. The data on spanwise planes contain U, V, and W data requiring that the measurements be performed twice (once for UV- and again for UW-orientations of the crossed-wire). The spanwise planes consist of a uniform 10mm × 10mm horizontal grid at a fixed Y=10mm containing 126 points in X and 41 points in Z (5166 grid points) and eight spanwise planes normal to the wall, each consisting of 41 points in Z and 17 points in Y. These measurements at 26,554 grid points required about 25 days of continuous operation (including hot-wire calibrations etc.) of the automated facility. The averages at each point were derived from 25,600 samples taken at 1024Hz corresponding to the passage of 200 disturbances. Temporal mean velocity and Reynolds stress measurements have also been obtained without the disturbance (i.e natural transition) to examine the effect of introducing the disturbance. The same streamwise and horizontal grids were used while only five of the spanwise

planes normal to the wall were needed for the comparison. These 2D slices through the measurement volume originate just upstream of the region of rapid growth of the instabilities.

Normal hot-wires can be positioned very close to the wall, and this makes them superior to crossed-wires for measuring the thin laminar velocity profiles ($\delta = 6 \rightarrow 10$ mm). Also, the effects of high shear are almost negligible, and they are less susceptible to error in regions of high turbulence intensity. Phase-averaged normal hot-wire data have been measured on 42 spanwise planes at 10mm intervals along the test-section from just upstream of the disturbance to about 0.2m downstream of the transition region.

4.3 Development of laminar layer in the favorable pressure gradient

The incoming profiles have inflection points close to the wall, presumably caused by the APG near the exit of the contraction. These inflection points disappear with streamwise distance and a self-similar profile shape is observed over about 15δ towards the end of this region. The FPG also has another beneficial effect of increasing the spanwise uniformity of the layer. Measurements with a Pitot tube resting on the wall were used to study the spanwise uniformity of the layer. The measurements were uniform to within $\pm 3\%$ over a spanwise distance of about 35δ. It is interesting to note that an inflection point develops in the laminar layer about 10mm upstream of the C_p minimum. The observations suggest that a Falkner and Skan similarity solution would adequately describe the layer in this region if an equivalent X and β (wedge angle) can be found. This would form a suitable starting point for an analytical or numerical study of the instability.

4.4 Development of laminar layer in the adverse pressure gradient

The closely spaced velocity profiles in figure 5 show the growth of strong inflection points leading to the formation of a shear layer. Development of the perturbation velocity with streamwise distance is shown in figure 6. Directly above the hole, the disturbance penetrates only 1mm into the layer (δ=6mm), and it has a maximum amplitude of -3% of U_∞. Small magnitude high frequency positive oscillations are also observed in time, but these are probably the result of transient mechanical vibrations in the shaker-diaphragm-tube system used to inject the disturbance. These positive oscillations decay rapidly with streamwise distance and disappear by 20mm downstream of the hole. The size of the perturbation continues to decay with streamwise distance reaching a minimum value 80mm downstream of the hole. At this streamwise location, the disturbance has the appearance of a short duration isolated sine-wave with a magnitude 0.15% U_∞. By about 150mm downstream of the hole, the disturbance starts to undergo rapid growth and complex phase relations begin to emerge between the signals obtained at different distances from the wall.

4.5 Transition region

The evidence suggests that the laminar layer eventually separates and that the transition mechanism is a shear-layer instability. The contours of spanwise vorticity

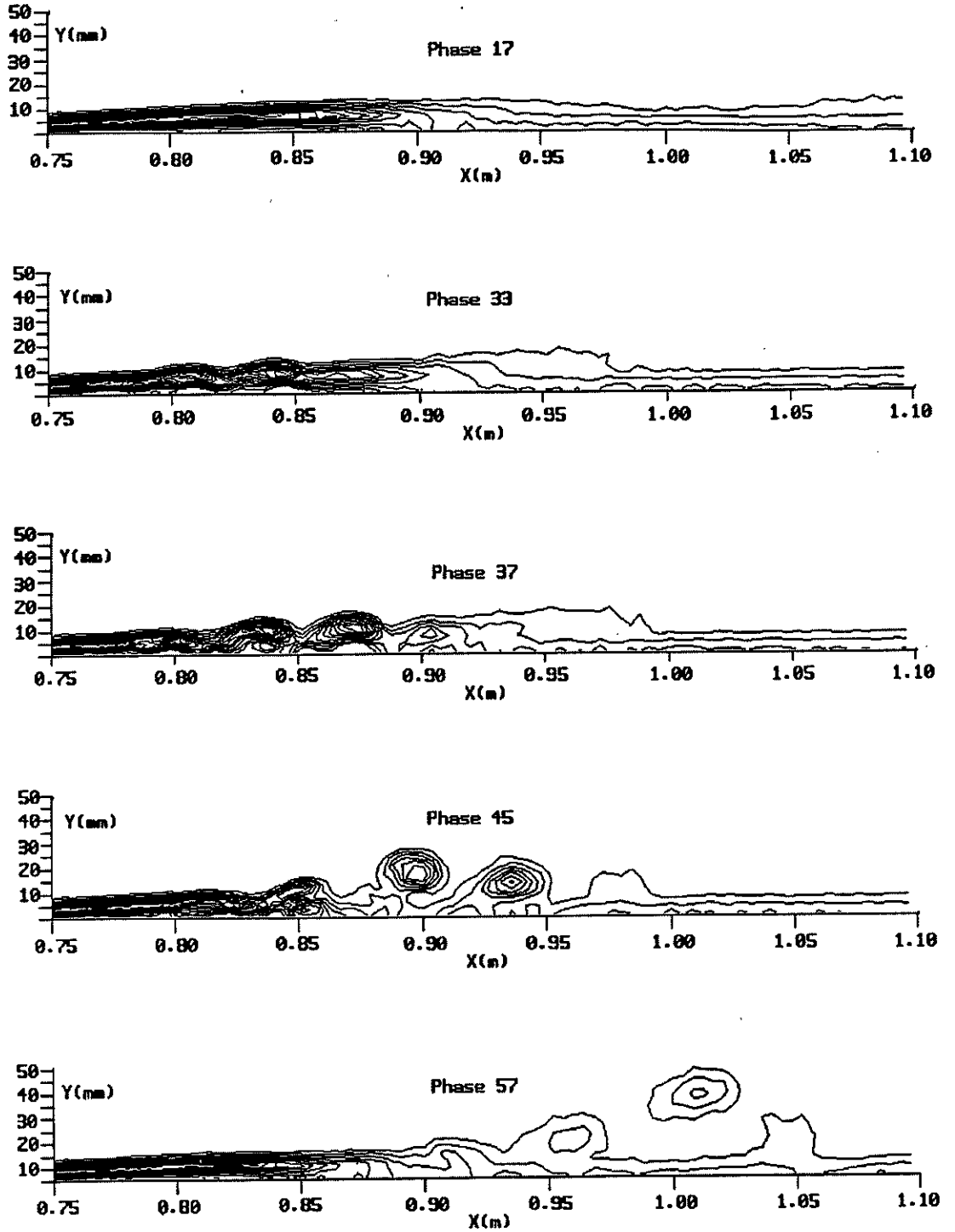

FIGURE 7. Selected phases showing roll-ups reminiscent of a free shear layer and their subsequent interaction with the wall.

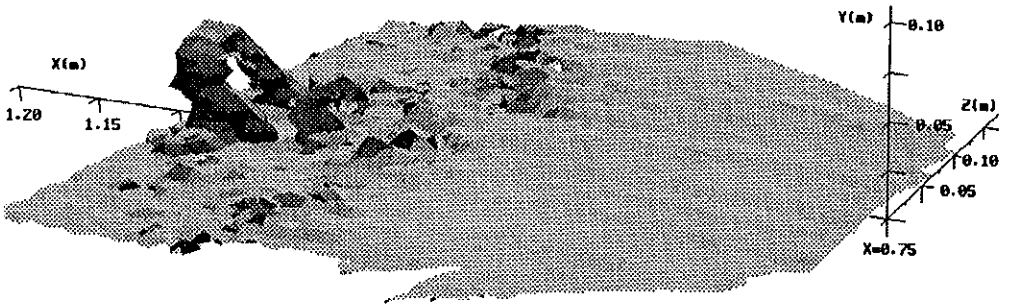

FIGURE 8. Contour surface of vorticity magnitude showing the vortex loops just downstream of the transition region.

in figure 7 show the formation of roll-ups which are reminiscent of a free shear layer. Four distinct spanwise vortex-like motions emerge, but subsequent interaction with the wall eventually leads to rapid growth of the second vortex. Smaller-scale vortex-like motions are also observed to propagate through the spanwise planes normal to the wall. In the horizontal plane, the region of large phase-averaged velocity perturbations has a wedge shape which is reminiscent of a turbulent spot. (It should be noted that the surrounding flow is turbulent, so using the term "turbulent spot" does not strictly conform to prior usage of the term.) The evolution of the "spot-like" flow pattern is slightly asymmetrical, and the large vortex-like motions become slightly displaced to one side of the centerline.

This region has recently been mapped out on a 3D (45×17×41) point grid in XYZ with greater spatial resolution. The 31,365 grid points were measured twice using both orientations of the crossed-wire probe to obtain U, V, and W data (as well as the Reynolds stresses at constant phase). Animation sequences of surfaces of constant vorticity magnitude show the formation of 3D waves which ultimately evolve into the large-scale vortex loops as shown in figure 8. At this stage, it is not clear whether smaller vortex-loops form as well. Visualization of the data is extremely difficult because the 3D contour surfaces are not transparent. Volume rendering techniques (transparency) are being explored as a means of examining the data. The spanwise propagation of the phase-averaged pattern is extraordinarily rapid, i.e. the spot-like flow expands to the ±0.2m width of the measurement grid (or greater) after streamwise development of about one only spot-length ($\approx$ 0.15m). Details of the organized motion gradually become "lost", and the phase-averaged contribution of the Reynolds stress falls to a relatively small fraction of the temporal mean value.

4.6 Downstream turbulent boundary layer

By about 0.5m downstream of the transition, the mean flow begins to develop

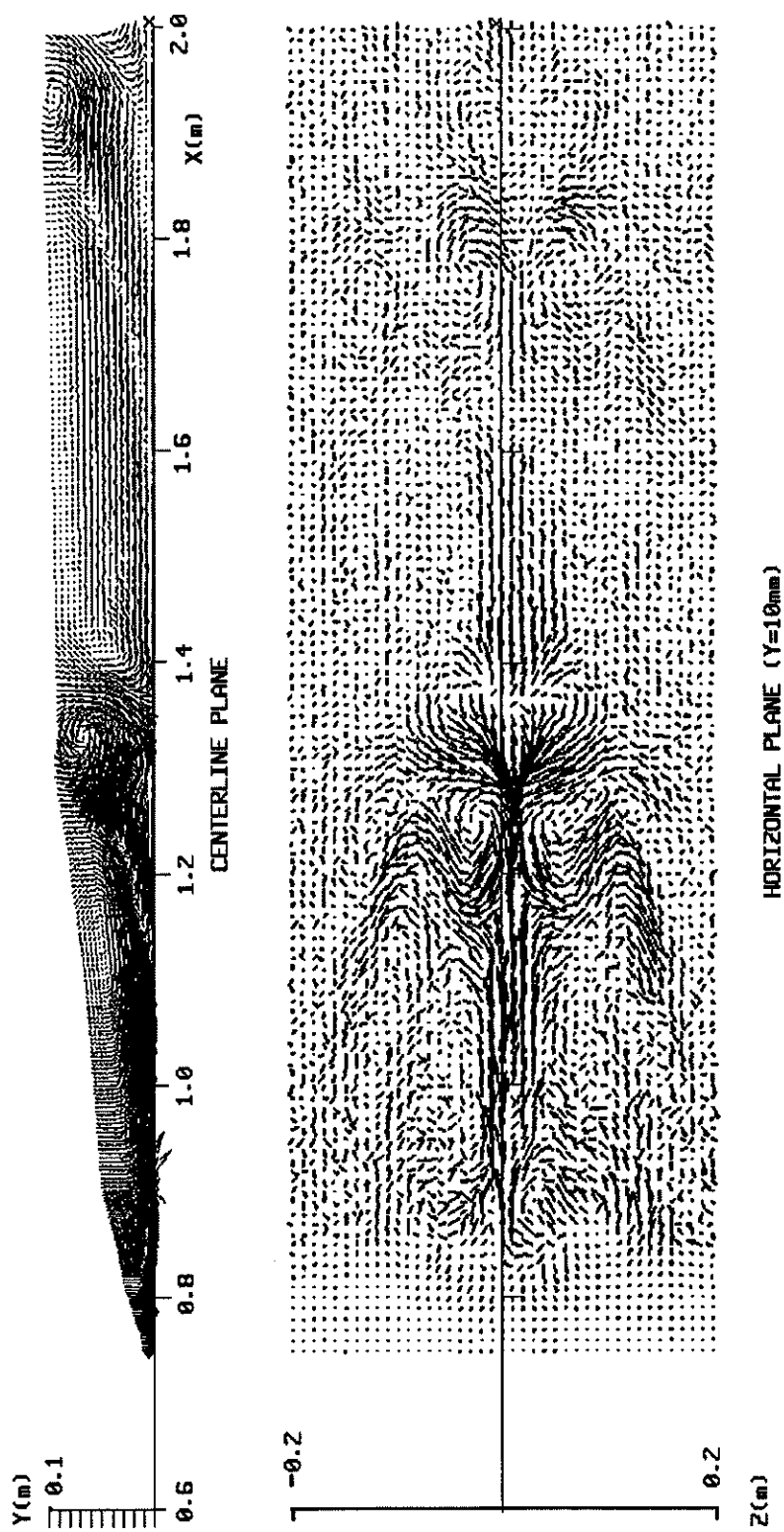

FIGURE 9. The large-scale vortex-loop that forms in the transition region retains its identity downstream in the turbulent boundary layer all the way to the end of the test-section.

many of the characteristics of a turbulent boundary layer. The individual vortex-like motions observed in the centerline plane appear to decay and merge into a single large eddy. Phase-averaged velocity vectors in the spanwise planes indicate that this large eddy has the form of a vortex-loop, similar in appearance but larger than the loop observed in the turbulent boundary layer study. Remarkably, the vortex loop remains visible in the velocity vector fields all the way to the end of the measurement grid (1.25m downstream of the point of transition) despite the interaction with the surrounding turbulent boundary layer, as shown in figure 9. In the horizontal plane, the two legs of the vortex loop have the appearance of two vortices of opposite sign which define the front edge of the spot-like flow. The edges of the spot-like structure can be observed where there are gradients of the phase-averaged velocities. This is probably the result of phase jitter, i.e. smearing of vorticity in the phase-averaging process.

5. Plans for future work on turbulent spots

The pressure distribution used for the transition study is rather arbitrary in the sense that it was designed to establish the DNS validation turbulent boundary layer. The laminar profiles in the APG are far from self-similar, and the APG is severe enough to cause separation. An APG distribution will be designed to produce closely self-similar laminar profiles. The advantage of self-similar profiles is that classical 2D linear stability theory can be used. The Reynolds number and the strength of the APG will be tuned by trial-and-error to see if a more conventional "spot-like" flow can be established. An important constraint is that the formation of spots occurs repetitively. Without this feature, the phase-averaging technique cannot be used. The automated facility will be used to obtain measurements on large 3D grids to examine the internal structure of the spot in detail.

The work was performed in the Fluid Mechanics Laboratory (FML) at NASA Ames Research Center. The project was partially supported by the FML.

REFERENCES

CANTWELL, B. J. & COLES, D. 1983 An experimental study of entrainment and transport in the turbulent near wake of a circular cylinder. *J. Fluid Mech.* **136**, 321-374.

CANTWELL, B. J., COLES, D. & DIMOTAKIS, P. 1978 Structure and entrainment in the plane of symmetry of a turbulent spot. *J. Fluid Mech.* **87**, 641-672.

EMMONS, H. W. 1951 The laminar-turbulent transition in a boundary layer. *J. Aero. Sci.* **18**, 490.

KOVAZNAY, L. S. G., FUJITA, H. & LEE, R. L. 1974 Unsteady turbulent puffs. *Advances in Geophysics.* **B18**, 229.

PERRY, A. E. & CHONG, M. C. 1982 On the mechanism of wall turbulence. *J. Fluid Mech.* **119**, 173-218.

PERRY, A. E., LIM, T. T. & TEH, E. W. 1981 A visual study of turbulent spots. *J. Fluid Mech.* **104**, 285.

PERRY, A. E. & WATMUFF, J. H. 1981 Phase-averaged large-scale structures in three-dimensional turbulent wakes. *J. Fluid Mech.* **103**, 33-51.

REYNOLDS, W. C. & HUSSAIN, A. K. M. F. 1972 The mechanics of a an organized wave in turbulent shear flow. Part 3. Theoretical models and comparison with experiments. *J. Fluid Mech.* **54**, 263.

SCHUBAUER, G. B. & KLEBANOFF, P. S. 1956 Contributions on the mechanics of boundary layer transition. *N.A.C.A. Rep. 909.*

WATMUFF, J. H. 1989 An experimental investigation of a low Reynolds number turbulent boundary layer subject to an adverse pressure gradient. *CTR Annual Research Briefs.* Center for Turbulence Research, Stanford University. 37-49.